Sensitivity of electron and electron-positron momentum densities to various electron and positron crystal potentials

H. Sormann
Institut für Theoretische Physik, Technische Universität Graz, Petersgasse 16, A-8010 Graz, Austria

M. Šob
Institute of Physics of Materials, Academy of Sciences of the Czech Republic, Žižkova 22, CZ-616 62 Brno, Czech Republic

(Received 12 July 2000; revised manuscript received 13 February 2001; published 28 June 2001)

This paper presents a comprehensive survey of the influence of various crystal potentials used for the calculation of electron and positron Bloch states on electron and electron-positron momentum densities. Our investigation deals with alkali metals and the complete series of $4sp$ and $3d$ metals, and it covers the behavior of both valence and core electrons as well as the central momentum region and some umklapp regions. The main results of this paper are the following: (i) The sensitivity of the electron-positron momentum density with respect to various crystal potentials is significantly higher for $4sp$ and $3d$ metals than for alkali metals. (ii) For all metals of the $3d$ series, the electron-positron momentum densities are generally more sensitive to the potentials than the corresponding electron momentum densities. Possible complications regarding the comparison of theoretical and experimental electron-positron momentum profiles, and means for extracting information on electron-positron interaction, are also discussed.

DOI: 10.1103/PhysRevB.64.045102 PACS number(s): 71.20.−b, 71.45.Gm, 71.60.+z, 78.70.Bj

I. INTRODUCTION

This paper reports on a consequent continuation of our previous work regarding the sensitivity of theoretically obtained electron momentum densities (EMD) and electron-positron momentum densities (MDAP) with respect to the crystal potentials which are used for the calculation of the electron and positron Bloch wave functions.[1,2]

In the present work, we continue and extend these calculations in the following directions: (i) we investigate the sensitivity behavior of EMD and MDAP-IPM [i.e., within the independent particle model (IPM)] for the complete series of $4sp$ and $3d$ metals [the metals with atomic numbers 19 (K) to 30 (Zn)]. (ii) Our calculations do not deal only with the valence part of the momentum densities as in Refs. 1 and 2, but also include the contribution of (at least the energetically highest) core states (in order to present a complete overview on the effects to be studied, our previous results on alkali metals[1,2] and results of other studies[3] are also included into the discussion). (iii) We present results regarding the calculation of the MDAP beyond the IPM, i.e., including electron-positron correlations.

As described in detail in Sec. II of this paper, our investigation into the sensitivity of EMD and MDAP profiles in metals is based on the use of three different electron and positron crystal potentials, namely, on the Mattheiss potentials[4] and on two particular self-consistent potentials, one of them including the local-density approximation of the exchange-correlation potential based on the work of Ceperley and Alder,[5] and another one including only Slater's exchange potential. It should be emphasized that it is not the purpose of this paper to decide if one of these potentials is ''better'' than the others. The main aspect which we want to demonstrate is that even small differences between the potentials may lead to considerable changes in the EMD and MDAP results. This may complicate or even prevent a reliable comparison of theoretical and experimental results. For example, in order to test various approaches for a theoretical description of electron-positron enhancement factors, and other differences, caused, e.g., by various approximations of the exchange-correlation part of the potentials etc., there may be sources of similar uncertainties in the theoretically obtained momentum densities. During the last years, such investigations have become even more important due to the development of effective numerical techniques enabling a more and more detailed and reliable reconstruction of densities based on two-dimensional angular correlation of positron annihiliation radiation (ACAR) projections.[6]

The paper is organized as follows: In Sec. II, we present a short review of the basic formulas of EMD and MDAP-IPM, and define the principal quantities for the present investigation. Section III contains the main results of our work, namely, a presentation and discussion of the differences between the three particular electron and positron crystal potentials used for this study (Sec. III A) and of the corresponding sensitivities of the EMD and MDAP (Sec. III B). In Sec. IV, it is illustrated by several examples how these potential-caused uncertainties of the momentum densities may ''mask'' differences of MDAP profiles due to various theoretical approaches to the electron-positron enhancement effect. Section V contains the conclusions of our investigations.

II. BASIC RELATIONS AND DEFINITIONS

The basic expressions of this study are the well-known formulas for the EMD,[7]

$$\rho_{\mathrm{e}}(\mathbf{p}) = \sum_{n\mathbf{k}} f(n,\mathbf{k})\,\delta(\mathbf{p}-\mathbf{k}-\mathbf{K}) \times \left| \frac{1}{\sqrt{\Omega}} \int_{\Omega} d^3r \exp(-i\mathbf{p}\cdot\mathbf{r})\,\psi_{n\mathbf{k}}(\mathbf{r}) \right|^2, \qquad (1)$$

and for the MDAP–IPM,[7]

$$\rho_{\mathrm{IPM}}(\mathbf{p}) = \sum_{n\mathbf{k}} f(n,\mathbf{k})\,\delta(\mathbf{p}-\mathbf{k}-\mathbf{K}) \times \left| \int_{\Omega} d^3r \exp(-i\mathbf{p}\cdot\mathbf{r})\,\psi_{n\mathbf{k}}(\mathbf{r})\,\psi_{+}(\mathbf{r}) \right|^2, \quad (2)$$

where $\hbar\mathbf{p}$ represents the electron or the electron-positron pair momentum, respectively, and $f(n,\mathbf{k})$ denotes the Fermi-Dirac distribution function for an electron state of band index n and (reduced) Bloch vector $\mathbf{k}$. The functions $\psi_{n\mathbf{k}}$ and ψ_{+} are the wave functions of an electron in the state $|n\mathbf{k}\rangle$ and of a thermalized positron, both normalized to unity in the volume of the Wigner-Seitz cell Ω. $\mathbf{K}$ denotes a reciprocal-lattice vector such that $\mathbf{p}-\mathbf{K}$ lies in the first Brillouin zone. Equations (1) and (2) give the EMD and MDAP *per spin direction*, i.e., without a factor 2 for the spin degeneracy. The quantity ρ_{e} is normalized such that

$$\frac{2\Omega}{(2\pi)^3 N} \sum_{\mathbf{G}} \int_{\mathrm{BZ}} d^3k\, \rho_e(\mathbf{k}+\mathbf{G}) = 1,$$

where $\mathbf{G}$ is a reciprocal-lattice vector, and N means the number of core and valence electrons per atom taken into account. In Secs. II and III, we deal exclusively with electron-positron momentum densities *within the independent-particle model*. Therefore, in these sections, we write simply MDAP for MDAP-IPM.

The electron and positron wave functions $\psi_{n\mathbf{k}}(\mathbf{r})$ and $\psi_{+}(\mathbf{r})$ are solutions of the one-particle Schrödinger-like equations

$$\left[-\frac{\hbar^2}{2m}\Delta + V_e(\mathbf{r}) \right] \psi_{n\mathbf{k}}(\mathbf{r}) = E_{n\mathbf{k}}\,\psi_{n\mathbf{k}}(\mathbf{r})$$

and

$$\left[-\frac{\hbar^2}{2m}\Delta + V_p(\mathbf{r}) \right] \psi_{+}(\mathbf{r}) = E_{+}\,\psi_{+}(\mathbf{r}),$$

respectively, where $V_e(\mathbf{r})$ and $V_p(\mathbf{r})$ are the corresponding electron and positron crystal potentials. For the present paper, the following three electron crystal potentials have been used.

$V_e^{(M)}$: Non-self-consistent muffin-tin potentials based on Mattheiss' construction scheme,[4] i.e., on a superposition of atomic electron densities. For all *d*-band metals investigated in the present study, the atomic configuration $3d^{n-1}\,4s^1$ has been used, as it turned out that this configuration yields the band structures closer to the self-consistent ones (see Refs. 8 and 9). The exchange part of the potentials has been approximated according to Slater's formula.

$V_e^{(\mathrm{CA})}$: Self-consistent muffin-tin potentials, obtained by the conventional nonrelativistic augmented-plane-wave method. For the exchange-correlation part of the potentials, we used a local-density approximation based on correlation energy calculations by Ceperley and Alder[5] (CA) in the parametrized form of Vosko *et al.*[10]

$V_e^{(S)}$: Self-consistent muffin-tin potentials, where only the exchange part of the electron-electron interaction according to Slater's formula is taken into account, and correlation effects are completely neglected. The positron potentials $V_{\mathrm{p}}^{(M)}$, $V_{\mathrm{p}}^{(\mathrm{CA})}$, and $V_{\mathrm{p}}^{(S)}$ have been obtained by taking the corresponding electron potentials without the exchange-correlation terms, and by using the opposite sign compared to that for the electrons.

Here we would like to stress that we have chosen these three potentials as *examples* to investigate the influence of various approximations to crystal potentials frequently used in EMD and MDAP calculations, for example employing various electron exchange-correlation potentials or, for the positron crystal potential, the inclusion of an electron-positron correlation term (neglected in the present investigation). In this paper, we compare the following pairs of potentials: (CA,S) represents the comparison of two self-consistent potentials with different choices of the exchange-correlation (xc) part of the crystal potential of the electron. (M,S) represents the comparison of potentials including the same approximation of the xc part (namely, simply Slater's exchange), but without or including self-consistency. Consequently, the comparison of (CA,M) represents the combined influence of these two effects.

In order to characterize the sensitivity of the EMD and MDAP with respect to various crystal potentials, we may define the *relative deviation in the potential* by

$$\Delta V_t^{(\alpha,\beta)} \equiv \frac{\int_{\Omega} d^3r \left| V_{\mathrm{t}}^{(\alpha)}(\mathbf{r}) - V_t^{(\beta)}(\mathbf{r}) \right|}{\int_{\Omega} d^3r \left| V_t^{(\alpha)}(\mathbf{r}) \right|},$$

where t stands for e or p (electron or positron), and (α,β) means the potentials to be compared. Since all crystal potentials employed here are of the muffin-tin type, they are spherically symmetric inside the muffin-tin (MT) spheres with radius r_{MT} and constant in the interstitial region Ω_{out}. As the potential is determined up to an additive constant, we may shift it such that its constant value in Ω_{out} is equal to zero. However, if we compare two muffin-tin potentials, their shapes may be quite different and their average values in the interstitial space do not have to be the same. In addition to this, there is no absolute scale for the crystal potentials,[11] so that we do not know *a priori* how to adjust the compared potentials with respect to each other. Therefore, we better define the quantity ΔV_t as a function of the parameter η,

$$\Delta V_{\mathrm{t}}^{(\alpha,\beta)}(\eta) \equiv \frac{4\pi \int_0^{r_{\mathrm{MT}}} dr\, r^2 \left| V_t^{(\alpha)}(r) - V_{\mathrm{t}}^{(\beta)}(r) + \eta \right| + \Omega_{\mathrm{out}} |\eta|}{4\pi \int_0^{r_{\mathrm{MT}}} dr\, r^2 \left| V_t^{(\alpha)}(r) \right|}, \quad (3)$$

where η means the difference between the constant parts of the two potentials within Ω_{out}. We choose η that ΔV_{t} becomes a minimum; such a comparison seems to be more appropriate than just to set the averages of both potentials in the interstitial space to the same value, i.e., to put $\eta=0$ in Eq. (3). Therefore, all values of ΔV_t used in this work are based on this method.

The *relative deviation in the momentum densities* is defined by

$$\Delta\rho_{i,j}^{(\alpha,\beta)} \equiv \frac{\int d^3k |\rho_i^{(\alpha)}(\mathbf{k}+\mathbf{G}_j) - \rho_i^{(\beta)}(\mathbf{k}+\mathbf{G}_j)|}{\int d^3k\ \rho_i^{(\alpha)}(\mathbf{k}+\mathbf{G}_j)}, \qquad (4)$$

where ρ_i, for $i=e$ or where i is the IPM, is given by Eq. (1) or (2), (α,β) has the same meaning as in Eq. (3), and the integration in $\mathbf{k}$ space goes over the first BZ. The second subscript j takes the values 0 or U, indicating whether the calculation of $\Delta\rho$ is performed within the central momentum region $[\mathbf{G}_0=(000)]$ or within one of the nearest umklapp regions $[\mathbf{G}_U=(110)$ for bcc metals and $\mathbf{G}_U=(111)$ for fcc metals].

The main purpose of our work is to investigate how the quantities $\rho_e(\mathbf{p})$ (EMD) and $\rho_{\text{IPM}}(\mathbf{p})$ (MDAP) are influenced by changes in the electron potential V_e. Therefore, the proper basis for all further discussions are the ratios

$$\Delta\rho_e/\Delta V_e \quad \text{and} \quad \Delta\rho_{\text{IPM}}/\Delta V_e, \qquad (5)$$

defined by the Eqs. (3) and (4), which describe the response of ρ_e and ρ_{IPM} to a *unit change* in the electron potential. We call these quantities the *sensitivities* of the EMD and MDAP with respect to V_e.

III. RESULTS AND DISCUSSION

In this section, we discuss the deviations ΔV_e and ΔV_p in the crystal potentials according to Eq. (3) and the sensitivity of the momentum densities according to Eq. (5). All investigations presented in this paper have been performed for Li, K, and Cs as representatives of the alkali metals, and for the metals of the $4sp$ and $3d$ group with atomic numbers from 19 (potassium) to 30 (zinc). Most of these metals have the body-centered-cubic (bcc) or the face-centered cubic (fcc) crystal structure; Sc, Ti, Co, and Zn, with their hexagonal close-packed (hcp) structure, are also treated as fcc metals with the same atomic volume as in the hcp case. Some basic quantities of the metals investigated in our work are given in Table I.

TABLE I. Basic information on the metals investigated in this paper. Z is the atomic number, and a is the lattice constant in a.u.

	Z	structure	a
Li	3	bcc	6.597
K	19	bcc	9.882
Cs	55	bcc	11.423
K	19	bcc	9.882
Ca	20	fcc	10.56
Sc	21	fcc [a]	8.772
Ti	22	fcc [a]	7.812
V	23	bcc	5.7145
Cr	24	bcc	5.4519
Mn	25	fcc	6.909
Fe	26	bcc	5.4169
Co	27	fcc [a]	6.686
Ni	28	fcc	6.6590
Cu	29	fcc	6.8308
Zn	30	fcc [a]	7.43

[a]Denotes a hcp metal which is treated as a fcc metal.

A. Deviations in the crystal potential

Our results of ΔV_e [Fig. 1(a)] and ΔV_p [Fig. 1(b)] show an interesting behavior. To start the discussion with ΔV_e for the alkali metals investigated, these values lie approximately between 0.038 and 0.047 for $\Delta V_e^{(\text{CA},M)}$ and $\Delta V_{\text{e}}^{(\text{CA},S)}$, and between 0.007 and 0.014 for $\Delta V_e^{(M,S)}$, which means that these electron potentials are much more sensitive to the choice of the xc potential than to the self-consistency process.

However, for the $3d$ metals investigated, the situation is considerably more complicated. We observe that the values of ΔV_e are generally smaller than for the alkali metals [especially for (CA,M) and (CA,S)], an effect which is obviously caused by the appearance of the d electrons. Apart from this fact, two different domains can be distinguished: at

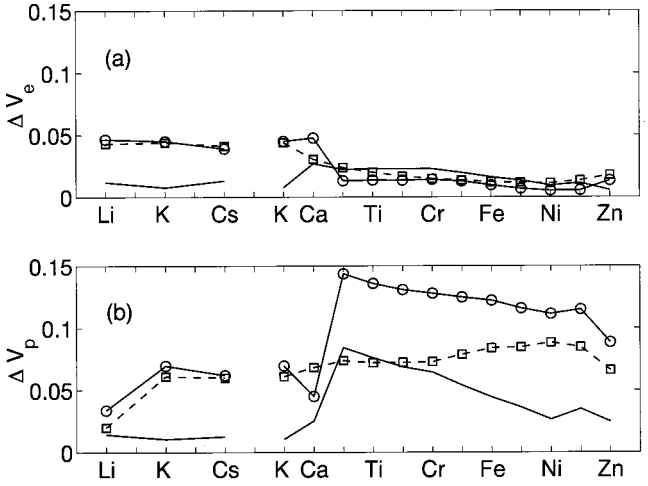

FIG. 1. Relative deviations of (a) electron and (b) positron crystal potentials for alkali metals (Li, K, Cs), calcium, and the series of metals from scandium to zinc. The values of η in Eq. (3) are chosen such that the deviations are minimum—see the discussion in the text. For clarity of the figure, only every second name of the series Ca→Sc→Ti→V→Cr→Mn→Fe→Co→Ni→Cu→Zn is indicated along the horizontal axis. Solid lines with circles: comparison of potentials (CA,M); dashed lines with squares: comparison of potentials (CA,S); solid lines: comparison of potentials (M,S).

the beginning (Sc, Ti) and the end of the $3d$ region except for Zn (Co, Ni, Cu), the values of both $\Delta V_e^{(\mathrm{CA},S)}$ and $\Delta V_e^{(M,S)}$ are quite similar, which shows that, for these metals, the effects of the choice of the xc potential and of self-consistency are of the same importance. As concerns the region between V and Fe, the dominant influence comes from self-consistency. Another interesting feature of the whole region of $3d$ metals (again, with the exception of Zn) is that the two deficiencies of the Mattheiss potentials, coming from their non-self-consistency and the neglect of the correlation potential, partly compensate, resulting in a surprising similarity of the potentials $V_e^{(\mathrm{CA})}$ and $V_e^{(M)}$.

This behavior of ΔV_e could mislead us into the obvious conclusion that, in accordance with Mattheiss' procedure for calculating the electron and positron crystal potential, this construction method is the more reliable the greater the number of relatively tightly bound electrons (d-electrons) included in the calculation.

However, as we learn from our results for ΔV_p [Fig. 1(b)], this argumentation is too simple. While the values of ΔV_e and ΔV_p are similar for the alkali metals, they behave completely differently for the d-band metals. This effect is not only quantitative (generally, all ΔV_p are significantly larger than the corresponding values of ΔV_e), but even qualitative, as we can see from the reversed order of the curves for $\Delta V^{(\mathrm{CA},M)}$ and $\Delta V^{(M,S)}$ in the electron and positron case. To be able to explain this different behavior, we performed detailed investigations where we separately calculated the deviations of both the Hartree part and the xc part of the electron potentials. It turns out that both deviations are—especially for d-band metals—of similar magnitude but different sign, and the resulting compensation effect is responsible for the observed small values of ΔV_e. However, for the positron potentials, such a compensation is no more effective due to the nonexistence of exchange and (at least in our approximation) correlation terms, which consequently leads to the large values of ΔV_p shown in Fig. 1(b).

B. Sensitivities of the EMD and MDAP

We are now going to discuss the sensitivities of the EMD and MDAP with respect to the changes in the electron potential ΔV_e. These quantities [defined by Eq. (5)] have been calculated both for the central momentum region [$\mathbf{G}=(000)$] and for the nearest umklapp regions centered around the reciprocal-lattice vectors $\mathbf{G}=(110)$ for bcc metals and $\mathbf{G}=(111)$ for fcc metals. In all EMD and MDAP calculations performed for this paper, we took into account the (occupied) valence states and the (energetically) highest core states of the electrons. To be specific, we considered $2s$, $4s$, and $6s$ valence bands for Li, K, and Cs, respectively, the $4s$ band for Ca, and the $3d$ and $4s$ bands for the series of metals from Sc to Zn. What concerns the core states included into our study, we took the $1s$ state for Li, the $3s$ and $3p$ states for K, and the $5s$ and $5p$ states for Cs. For all metals from Ca to Zn, the $3s$ and $3p$ core states have been taken into account. Here and henceforth in this paper, we use the following terminology: the values of $\Delta\rho_{i,j}/\Delta V_e$ which include only the *valence* (*core*) electrons are called the *valence (core)* sensitivities, and the values of $\Delta\rho_{i,j}/\Delta V_e$ which include *all* electrons represent the *total* sensitivities.

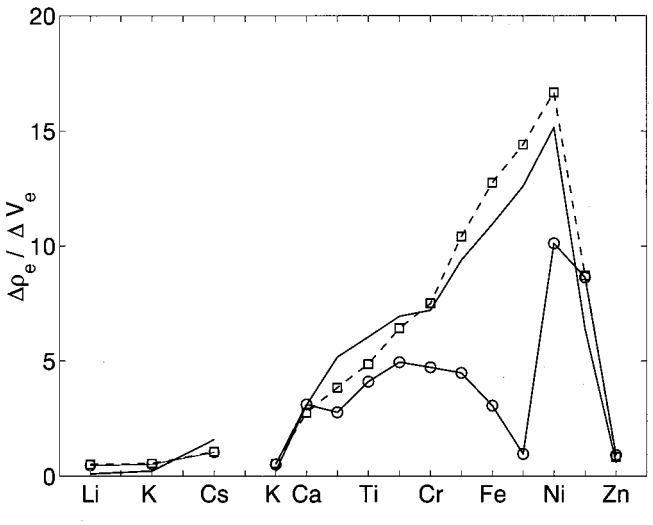

FIG. 2. *Valence* sensitivities $(\Delta\rho_{e,0}/\Delta V_e)^{\mathrm{val}}$ in the central momentum region for the EMD in alkali metals (Li, K, Cs), calcium, and the series of metals from scandium to zinc. The meaning of the three curves and the notation of the horizontal axis is the same as in Fig. 1.

Let us start the discussion with the valence sensitivity of the EMD for the central momentum region (Fig. 2). For the alkali metals and for all cases investigated [(CA,M), (CA,S), and (M,S)], one observes small values for this quantity, with the tendency to increase with increasing atomic number: for example, $(\Delta\rho_{e,0}^{(\mathrm{CA},M)}/\Delta V_e)^{\mathrm{val}}$ amounts to 0.463 for lithium, 0.519 for potassium, and 1.036 for caesium, in agreement with our previously published results of Ref. 1.

Generally, for the $3d$ metals, the valence sensitivities are significantly higher than for the alkali metals, and, apart from this, a detailed interpretation of the sensitivity curves is more complicated. In order to discuss these results properly, it is necessary to remember that—in contrast to the alkali metals—more than one valence band contributes to the momentum density. If we separately investigate the EMD values of the *first* (energetically lowest) valence band and the *higher* valence bands, we learn that the individual contributions to $\Delta\rho_e$ are quantitatively similar and of the opposite sign. For these reasons, we should expect a cancellation of the potential-caused deviations for the *first* and the *higher* bands resulting in small sensitivities of the EMD for the whole d-band region. However, this expectation is not fulfilled by the results for $(\Delta\rho_{e,0}^{(\mathrm{CA},S)}/\Delta V_e)^{\mathrm{val}}$ and $(\Delta\rho_{e,0}^{(M,S)}/\Delta V_e)^{\mathrm{val}}$ shown in Fig. 2. Conversely, we observe a monotonous increase of these quantities from K over Ca and all $3d$ metals up to nickel where remarkable values of 15 and more are reached, indicating that the EMD of the $3d$ metals is very sensitively influenced both by the xc part of the crystal potential and by the fact of whether the potential is self-consistent or not. The reason for this increase is that the *first* valence band is always completely occupied whereas—for most of the $3d$ metals—some of the higher bands intersect

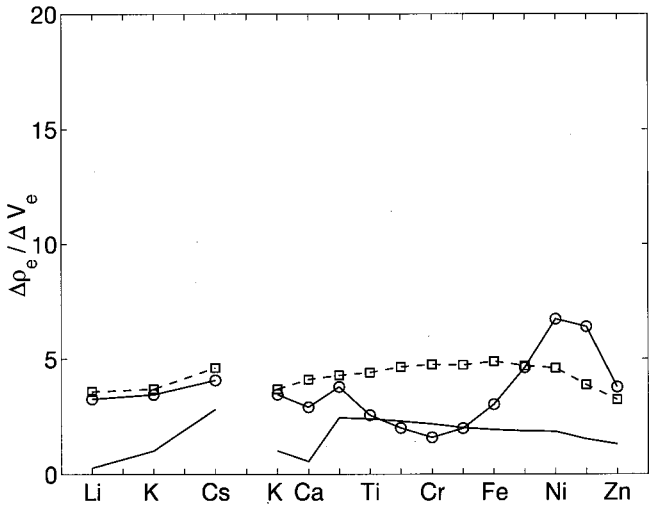

FIG. 3. *Core* sensitivities $(\Delta\rho_{e,0}/\Delta V_e)^{\text{core}}$ in the central momentum region for the EMD in alkali metals (Li, K, Cs), calcium, and the series of metals from scandium to zinc. The meaning of the three curves and the notation of the horizontal axis is the same as in Fig. 1.

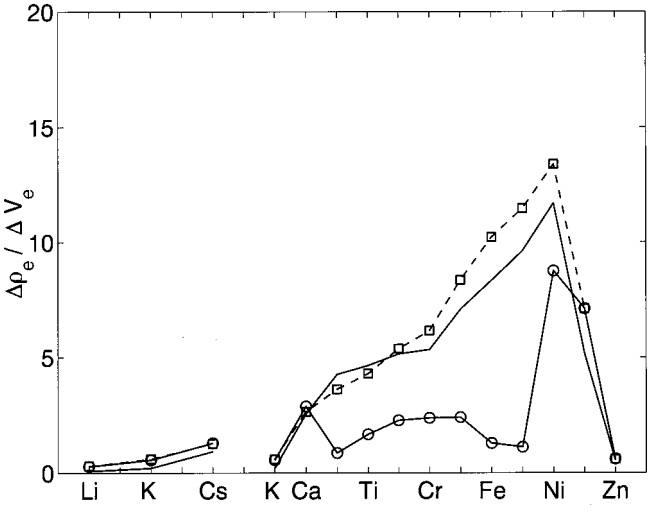

FIG. 4. *Total* sensitivities $(\Delta\rho_{e,0}/\Delta V_e)^{\text{total}}$ in the central momentum region for the EMD in alkali metals (Li, K, Cs), calcium, and the series of metals from scandium to zinc. The meaning of the three curves and the notation of the horizontal axis is the same as in Fig. 1.

the Fermi level and are therefore only partially occupied. Consequently, the cancellation effect mentioned above is *incomplete* for all metals from Sc to Ni; only for the last two metals investigated, copper and zinc, with their filled $3d$ shells, this compensation effect is *nearly* (Cu) or *completely* (Zn) perfect, which explains the abrupt decrease of the sensitivity curves in Fig. 2 for these metals.

Until now, we have not discussed the curve for (CA,M) in Fig. 2 with its relatively complicated shape. At first, we observe that, for all $3d$ metals from Sc to Ni, the sensitivity for (CA,M) is smaller than for (CA,S) and (M,S). This indicates a further compensation process, namely, between the effects of different xc-potentials and of self-consistency. Another strange feature of this curve is the decrease of $(\Delta\rho_e/\Delta V_e)^{(\mathrm{CA},M)}$ for Mn$\rightarrow$Fe$\rightarrow$Co, followed by a steep increase to Ni. As a result of numerous calculations, we obtained that this behavior is due to a change of the sign of the differences between $\rho_e^{(\mathrm{CA})}$ and $\rho_e^{(M)}$: $\rho_e^{(\mathrm{CA})} < \rho_e^{(M)}$ for all metals before Co, and $\rho_e^{(\mathrm{CA})} > \rho_e^{(M)}$ for all metals after Co, leading to the very small value of ≈ 0.97 for the sensitivity for this metal.

It is interesting that the core sensitivities for the alkali metals in the central momentum region (Fig. 3) are significantly higher (roughly by a factor of 4–7) than the corresponding valence sensitivities. The opposite is true for the $3d$ metals where $(\Delta\rho_{e,0}/\Delta V_e)^{\text{core}}$ is generally smaller than $(\Delta\rho_{e,0}/\Delta V_e)^{\text{val}}$. This is especially significant in the (M,S) case which reflects the well-known fact that the core contribution to the EMD is only weakly dependent on the fact if the crystal potential is self-consistent or not.

The total sensitivities in the central momentum region (Fig. 4) are qualitatively similar to the corresponding valence sensitivities. Quantitatively, the influence of the core electrons on $(\Delta\rho_{e,0}/\Delta V_e)^{\text{total}}$ is, of course, dependent on the fact how much the core electrons contribute to the total electron momentum density. For the alkali metals and calcium, this contribution is very small for $\mathbf{G}=(000)$. Therefore, the values of the total and the valence sensitivity are quite similar. However, for the $3d$ metals, the role of the core electrons is more important, which leads to a significant reduction of the values of $(\Delta\rho_{e,0}/\Delta V_e)^{\text{total}}$ compared to $(\Delta\rho_{e,0}/\Delta V_e)^{\text{val}}$. This effect is especially pronounced for the (CA,M) sensitivities in the region from Sc to Fe, where the values of the total sensitivity are by a factor of 2–3 smaller than those of the valence sensitivity.

The valence sensitivities of the EMD within the nearest umklapp region are presented in Fig. 5. Compared to the corresponding results for $\mathbf{G}=(000)$, one observes a consid-

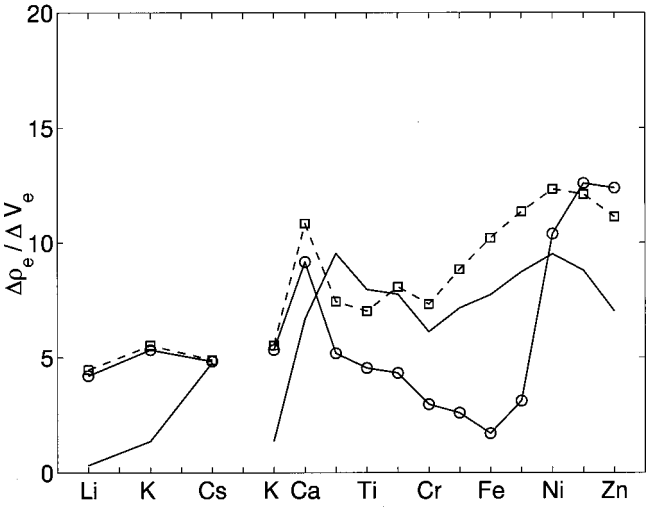

FIG. 5. *Valence* sensitivities $(\Delta\rho_{e,U}/\Delta V_e)^{\text{val}}$ in the nearest umklapp momentum region for the EMD in alkali metals (Li, K, Cs), calcium, and the series of metals from scandium to zinc. The meaning of the three curves and the notation of the horizontal axis is the same as in Fig. 1.

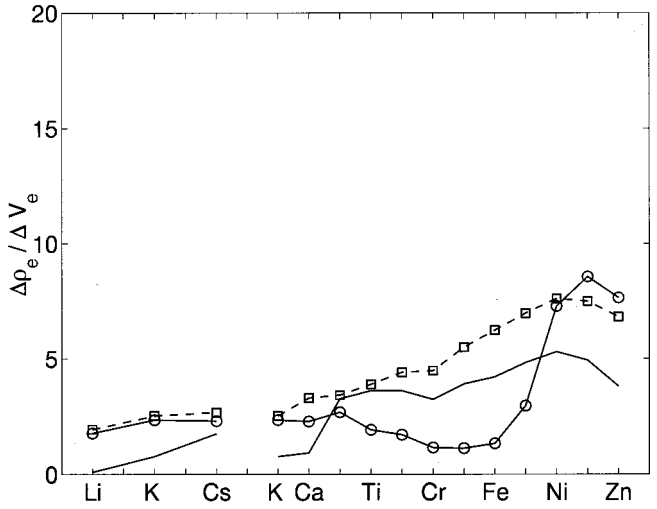

FIG. 6. *Total* sensitivities $(\Delta\rho_{e,U}/\Delta V_e)^{\text{total}}$ in the nearest umklapp momentum region for the EMD in alkali metals (Li, K, Cs), calcium, and the series of metals from scandium to zinc. The meaning of the three curves and the notation of the horizontal axis is the same as in Fig. 1.

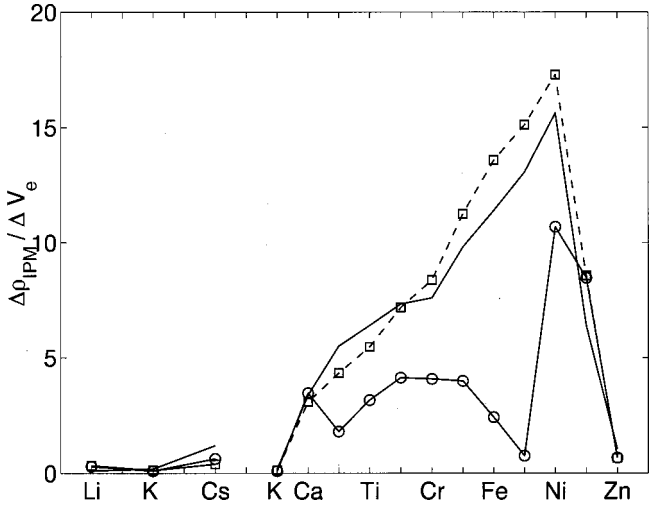

FIG. 7. *Valence* sensitivities $(\Delta\rho_{\text{IPM},0}/\Delta V_e)^{\text{val}}$ in the central momentum region for the MDAP-IPM in alkali metals (Li, K, Cs), calcium, and the series of metals from scandium to zinc. The meaning of the three curves and the notation of the horizontal axis is the same as in Fig. 1.

erable increase of this quantity for the alkali metals and calcium (a result discussed in detail in Ref. 1), whereas the sensitivities of the *d*-band metals are roughly of the same magnitude. What concerns the core sensitivity, our results for $\mathbf{G}=(110)$ and $\mathbf{G}=(111)$ are significantly (by a factor of 1.5–2) smaller than their counterparts for $\mathbf{G}=(000)$. On the other hand, the contribution of the core electrons to the EMD in the umklapp region is significantly more important than in the central momentum region. This leads to a strong reduction of the total sensitivity (Fig. 6) compared to the valence sensitivity (Fig. 5) for all metals investigated.

We are now going to study how the inclusion of a positron changes the results discussed above. For this purpose, in Figs. 7–10, we present some of our results regarding valence and total sensitivities of the MDAP to the electron crystal potential.

The influence of the positron on the valence sensitivity in the central momentum region can be discussed by comparing the MDAP results (Fig. 7) with the corresponding EMD values (Fig. 2): for the alkali metals, one observes a significant decrease of this quantity (a result which we have already arrived at in Ref. 1). For the *d*-band metals, however, this influence is smaller and by no means uniform, i.e., it changes from a moderate *decrease* in the (CA,M) case to a small *increase* for (CA,S). We are not able to explain this behavior in detail; all we can say is that these (small) changes of the sensitivity values depend on the shape of the positron wave function for the individual metals.

A general effect due to the positron is the well-known decrease of the core contribution to the MDAP (compared to the EMD), caused by the small annihilation probability of the positron with the core electrons. The reduced influence of these electrons is impressingly documented in Figs. 7 and 8: unlike the situation for the EMD, the core electrons hardly contribute to the electron-positron momentum density, leading to rather similar curves for the valence and the total sensitivity, both qualitatively and quantitatively. For example, in the case of nickel, the values of the total sensitivity for (CA,S) and (M,S) are only reduced by 7.9% and 5.9%, respectively, compared to the valence sensitivity. For the EMD, the corresponding numbers are 24.6% and 29.6%. Another striking example for the small influence of the core electrons on the sensitivity of the MDAP is the behavior of vanadium, chromium, and manganese: the corresponding values of $(\Delta\rho^{(\mathrm{CA},M)}_{\text{IPM},0}/\Delta V_e)^{\text{total}}$ and $(\Delta\rho^{(\mathrm{CA},M)}_{\text{IPM},0}/\Delta V_e)^{\text{val}}$ agree within 1–5 %, whereas, in the case of the EMD, one observes differences of 46–54 %. From the point of view of positron physics, the most important (and unpleasant) conse-

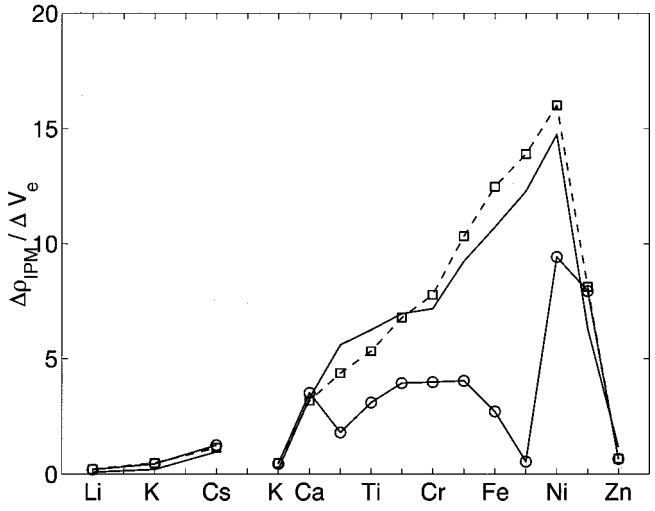

FIG. 8. *Total* sensitivities $(\Delta\rho_{\text{IPM},0}/\Delta V_e)^{\text{total}}$ in the central momentum region for the MDAP-IPM in alkali metals (Li, K, Cs), calcium, and the series of metals from scandium to zinc. The meaning of the three curves and the notation of the horizontal axis is the same as in Fig. 1.

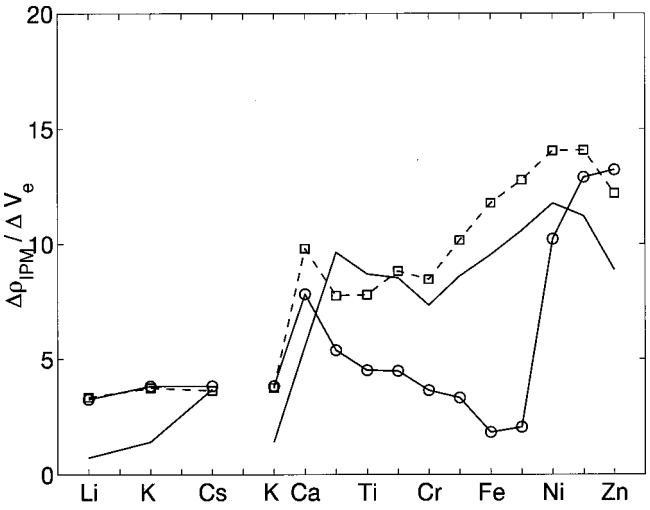

FIG. 9. *Valence* sensitivities $(\Delta\rho_{\mathrm{IPM},U}/\Delta V_e)^{\mathrm{val}}$ in the nearest umklapp momentum region for the MDAP-IPM in alkali metals (Li, K, Cs), calcium, and the series of metals from scandium to zinc. The meaning of the three curves and the notation of the horizontal axis is the same as in Fig. 1.

quence of this situation is that, for the *d*-band metals, the sensitivity of the MDAP to crystal potentials is in most cases significantly higher than for the EMD.

Finally, if we compare the valence sensitivity of the MDAP in umklapp regions (Fig. 9) with the corresponding values of the total sensitivity (Fig. 10), we observe the following two effects: on the one hand, the core contribution to the momentum density is large in the high-momentum region. On the other hand, the reduction of this core influence due to the positron is also quite efficient. Consequently, the total sensitivities are smaller than the corresponding valence

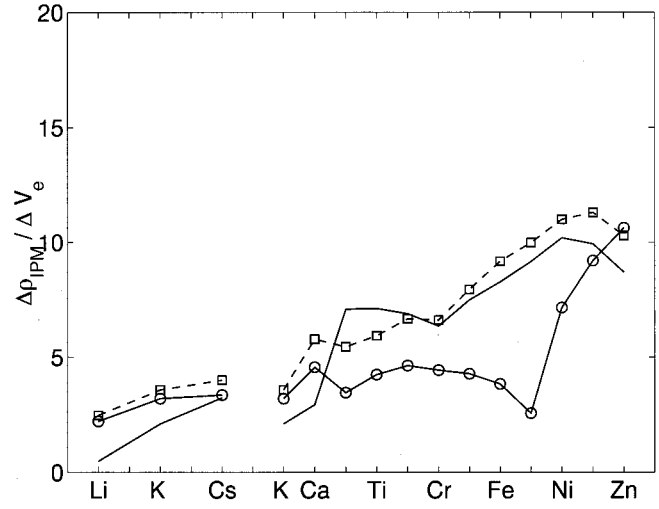

FIG. 10. *Total* sensitivities $(\Delta\rho_{\mathrm{IPM},U}/\Delta V_e)^{\mathrm{total}}$ in the nearest umklapp momentum region for the MDAP-IPM in alkali metals (Li, K, Cs), calcium, and the series of metals from scandium to zinc. The meaning of the three curves and the notation of the horizontal axis is the same as in Fig. 1.

sensitivities, but this effect is not as strong as in the EMD case.

IV. POTENTIAL EFFECTS IN CORRELATED MDAP PROFILES

As we already emphasized in the Sec. I, one of the main goals of this investigation is to demonstrate that the strong sensitivities of electron-positron momentum densities due to uncertainties of the crystal potentials (especially for *d*-band metals) may deteriorate the chance of a precise comparison between theoretical and experimental momentum profiles in order to assess the quality of various enhancement theories. As an illustration of this aspect, we finally present some theoretical electron-positron momentum density profiles where the effect of the Coulombic interaction between the annihilating particles is approximately described by the insertion of a *local* electron-positron pair correlation function g_{ep} into the MDAP-IPM formula [Eq. (2)] leading to the well-known *local-density approach* (MDAP-LDA)

$$\rho_{\mathrm{LDA}}(\mathbf{p})=\sum_{n\mathbf{k}} f(n,\mathbf{k})\,\delta(\mathbf{p}-\mathbf{k}-\mathbf{K})\left|\int_{\Omega} d^3r\,\exp(-i\mathbf{p}\cdot\mathbf{r})\right.$$
$$\left.\times\sqrt{g_{\mathrm{ep}}(\mathbf{r};n\mathbf{k})}\,\psi_{n\mathbf{k}}(\mathbf{r})\,\psi_{+}(\mathbf{r})\right|^2. \tag{6}$$

According to the proposal of Daniuk and co-workers,[12,13] g_{ep} can be taken from the enhancement theory of thermalized positrons within a homogeneous electron gas (see, e.g., Refs. 14 and 15), namely,

$$g_{\mathrm{ep}}(\mathbf{r};n\mathbf{k})=\epsilon_{\mathrm{hom}}[r_s(\mathbf{r});\chi_{n\mathbf{k}}] \tag{7}$$

with $r_s(\mathbf{r})=[4\pi n(\mathbf{r})/3]^{-1/3}$ and $n(\mathbf{r})$ as the total *local* density of the electron gas. Following the ideas of Sob[16–18] and, independently, of Mijnarends and Singru,[19] the quantity $\chi_{n\mathbf{k}}$ which describes the momentum-dependence of the enhancement factor can be considered an energy- and state-dependent function. However, despite the impressing success of the LDA, the physically most convincing form of $\chi_{n\mathbf{k}}$ is not clear. One of the first proposals for this quantity (see, e.g., Refs. 12, 13, 20 and 21, and discussions therein) reads

$$\chi_{n\mathbf{k}}(\mathbf{r})=\sqrt{[E_{n\mathbf{k}}-V_e(\mathbf{r})]/[E_F-V_e(\mathbf{r})]} \tag{8}$$

for $E_{n\mathbf{k}}-V_e(\mathbf{r})\leqslant 0$ and zero otherwise, where χ contains the *local* kinetic energy of the electrons. In Ref. 3, the form

$$\chi_{n\mathbf{k}}=\begin{cases}\sqrt{(E_{n\mathbf{k}}-E_0)/(E_F-E_0)} & E_{n\mathbf{k}}-E_0\geqslant 0\\ 0 & E_{n\mathbf{k}}-E_0<0\end{cases} \tag{9}$$

is proposed, with E_0 as the bottom energy of the electron conduction bands and E_{F} as the Fermi energy. The values of $\chi_{n\mathbf{k}}$ according to Eqs. (8) and (9) differ considerably for the valence electrons and are quite similar (namely, small or zero) for the core electrons.

Let us assume now that we want to compare the calculated positron annihilation profiles with experimental data to get out which of the two approaches to $\chi_{n\mathbf{k}}$ is the more appropriate one. In this case, we face the problem that the

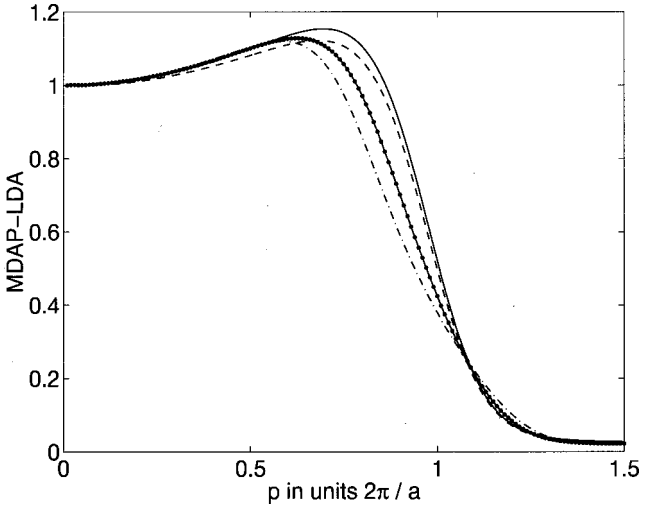

FIG. 11. Electron-positron momentum densities $\rho_{\mathrm{LDA}}(\mathbf{p})$, Eq. (6), in calcium along the [100] direction in momentum space. The enhancement effect is described by the local-density approximation (see Sec. IV). All curves are normalized to 1 at zero momentum. Solid line: CA electron and positron crystal potentials; local-density approximation according to Eq. (9). Dashed line: CA potentials; local-density approximation according to Eq. (8). Dash-dotted line: *M* potentials; local-density approximation according to Eq. (9). Full line with dots: *S* potentials; local-density approximation according to Eq. (9).

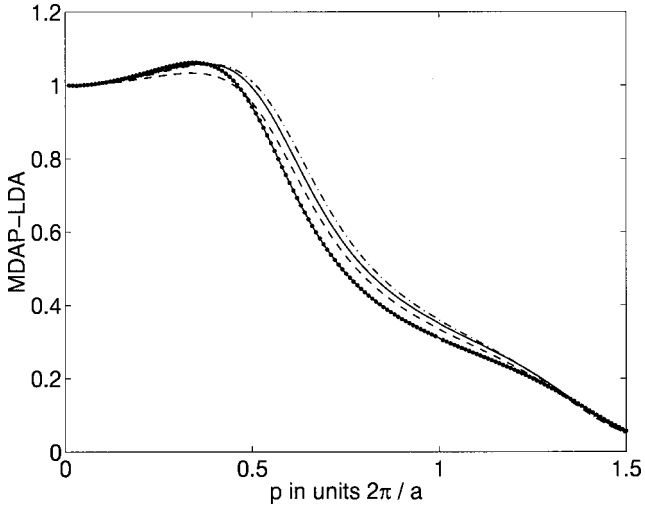

FIG. 13. Electron-positron momentum densities $\rho_{\mathrm{LDA}}(\mathbf{p})$ [Eq. (6)] in vanadium along the [100] direction in momentum space. The enhancement effect is described by the local-density approximation (see Sec. IV). All curves are normalized to 1 at zero momentum. The meaning of the four curves is the same as in Fig. 11.

effects of (i) different theoretical approximations for the electron-positron enhancement, and (ii) uncertainties of the theoretical results due to different electron and positron crystal potentials are often of the same order, which makes a reliable analysis of differences between theory and experiment problematic. This is demonstrated in Figs. 11–14, where we show LDA-enhanced electron-positron momentum densities for Ca, Sc, V, and Cu. All these figures contain four types of curves which are based on Eqs. (6) and (7) with different electron and positron crystal potentials and on different theoretical approaches to the enhancement [according to Eq. (8) or (9)].

Our results for calcium, scandium, and vanadium (Figs. 11–13) clearly show that the difference of the MDAP-LDA curves with respect to different theoretical approaches for the electron-positron pair-correlation function is significantly smaller than the difference due to different crystal potentials. As concerns the results for copper (Fig. 14), one observes a similar behavior for values of MDAP-LDA below the Fermi momentum in the first BZ. Above the Fermi momentum and in the umklapp region, the difference between the momen-

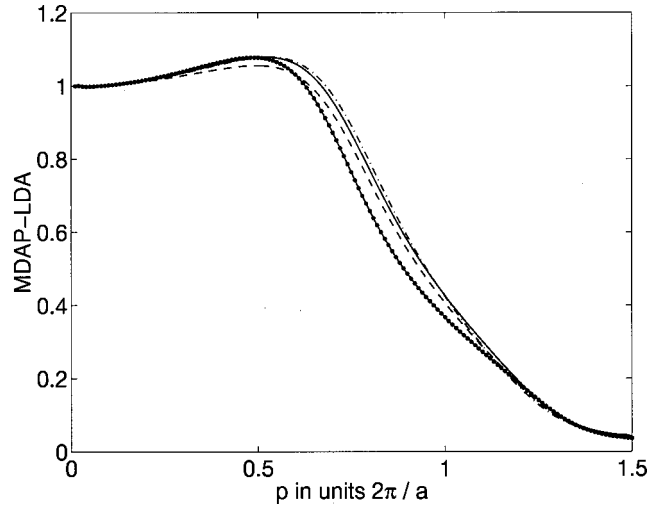

FIG. 12. Electron-positron momentum densities $\rho_{\mathrm{LDA}}(\mathbf{p})$ [Eq. (6)], in scandium along the [100] direction in momentum space. The enhancement effect is described by the local-density approximation (see Sec. IV). All curves are normalized to 1 at zero momentum. The meaning of the four curves is the same as in Fig. 11.

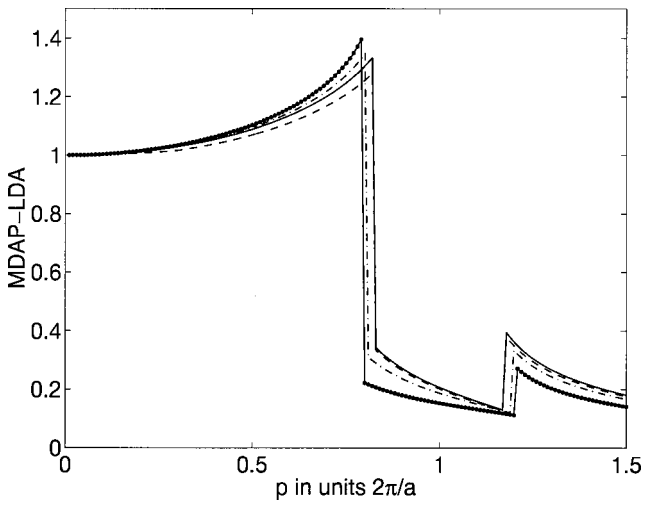

FIG. 14. Electron-positron momentum densities $\rho_{\mathrm{LDA}}(\mathbf{p})$ [Eq. (6)] in copper along the [100] direction in momentum space. The enhancement effect is described by the local-density approximation (see Sec. IV). All curves are normalized to 1 at zero momentum. The meaning of the four curves is the same as in Fig. 11.

tum densities belonging to Eqs. (8) and (9) for the electron-positron interaction is very small, and does not allow any critical examination of these two theoretical approaches.

V. CONCLUSIONS

The main topic of this paper is the sensitivity of the electron and the electron-positron momentum density in alkali metals and in $4sp$ and $3d$ metals with respect to various electron and positron crystal potentials. As the results and discussions presented in the previous sections have shown, this sensitivity is a rather complicated quantity which is not only different from metal to metal but is also strongly dependent on the momentum and on the special properties of the potentials to be used. Nevertheless, some principal statements can be formulated:

(i) In general, the EMD and MDAP in the $3d$ metals are significantly more sensitive to changes of the crystal potentials than the corresponding momentum densities in simple metals such as alkali metals, calcium, etc.

(ii) In many cases investigated, especially for the $3d$ metals, the values of the sensitivities are significantly smaller for the core electrons than for the valence electrons. Therefore, the sensitivities of the total momentum densities are reduced by the influence of the core electrons. Of course, this effect is the more important the more the core electrons contribute to the total momentum density, and it is, therefore, generally more efficient in the umklapp regions than in the central momentum region. Additionally, it is well known that the inclusion of the positron weakens the influence of the core electrons on the momentum density. This has the important consequence that the sensitivity of the MDAP is frequently larger than the corresponding sensitivity of the EMD, a statement which is valid both for the central momentum region and the Umklapp regions.

(iii) Quantitatively, the highest values of the sensitivity observed in our investigations appear for $3d$ metals in the first Brillouin zone if the crystal potentials differ by their exchange-correlation term. In this case, the total sensitivity amounts to 4.4 for scandium, 7.8 for chromium, and even 16.0 for nickel, remarkable values when compared to those for the alkali metals (0.2 for lithium up to 1.1 for cesium).

(iv) Such a strong sensitivity of theoretically obtained MDAP in metals with respect to various approximations of the crystal potential, especially in transition metals, may have far-reaching consequences. In fact, we can conclude from our results, in particular from those presented in Figs. 11–14, that a high sensitivity of the MDAP to the details of crystal potentials makes it very difficult or even impossible to use a comparison between theoretical and experimental momentum densities as a criterion to decide which electron-positron interaction theory is better. This is not very good news for theorists working in this field.

[1] H. Sormann and M. Šob, Phys. Rev. B **41**, 10 529 (1990).

[2] H. Sormann and M. Šob, Mater. Sci. Forum **105–110**, 841 (1992).

[3] S. Daniuk, M. Šob, and A. Rubaszek, Phys. Rev. B **43**, 2580 (1991).

[4] L.F. Mattheiss, Phys. Rev. **134**, A970 (1964).

[5] D.M. Ceperley and B.J. Alder, Phys. Rev. Lett. **45**, 566 (1980).

[6] Extensive information about *image reconstruction of momentum densities* (Cormack's method, filtered back projection methods, spherical harmonics reconstructions, inverse Fourier tranform methods, etc.) can be found in the literature. See, e.g., G. Kontrym-Sznajd and M. Samsel-Czekała, Appl. Phys. A: Mater. Sci. Process. **70**, 89 (2000).

[7] P.E. Mijnarends, Physica (Amsterdam) **63**, 235 (1973).

[8] E.C. Snow and J.T. Waber, Acta Metall. **17**, 623 (1969).

[9] P. Ziesche, H. Wonn, C. Müller, V.V. Nemoshkalenko, and V.P. Krivitskii, Phys. Status Solidi B **87**, 129 (1978).

[10] S.H. Vosko, L. Wilk, and M. Nusair, Can. J. Phys. **59**, 1200 (1980).

[11] W.R.L. Lambrecht, B. Segall, and O.K. Andersen, Phys. Rev. B **24**, 7412 (1981).

[12] S. Daniuk, G. Kontrym-Sznajd, J. Mayers, A. Rubaszek, H. Stachowiak, P.A. Walters, and R.N. West, in *Positron Annihilation*, edited by P.C. Jain, R.M. Singru, and K.P. Gopinathan (World Scientific, Singapore, 1985), p. 43; *ibid.*, p. 279.

[13] S. Daniuk, G. Kontrym-Sznajd, A. Rubaszek, H. Stachowiak, J. Mayers, P.A. Walters, and R.N. West, J. Phys. F: Met. Phys. **17**, 1365 (1987).

[14] A. Rubaszek and H. Stachowiak, Phys. Status Solidi B **124**, 159 (1984).

[15] A. Rubaszek and H. Stachowiak, Phys. Rev. B **38**, 3846 (1988).

[16] M. Šob, in *Proceedings of the 8th Annual International Symposium on the Electronic Structure of Metals and Alloys*, edited by P. Ziesche (Technische Universität Dresden, Dresden, 1978), p. 170.

[17] M. Šob, in *Positron Annihilation*, edited by R.R. Hasiguti and K. Fujiwara (The Japanese Institute of Metals, Sendai, 1979), p. 309.

[18] M. Šob, J. Phys. F: Met. Phys. **12**, 571 (1982).

[19] P.E. Mijnarends and R.M. Singru, Phys. Rev. B **19**, 6038 (1979).

[20] S. Daniuk, G. Kontrym-Sznajd, J. Majsnerowski, M. Šob, and H. Stachowiak, J. Phys.: Condens. Matter **1**, 6321 (1989).

[21] G. Kontrym-Sznajd and J. Majsnerowski, J. Phys.: Condens. Matter **2**, 9927 (1990).